The Finite Segment Method—A Numerical Rolling Contact Fatigue Life Model for Bearings Subjected to Stochastic Operating Conditions

Oliver Menck
Fraunhofer Institute for Wind Energy Systems IWES,
Am Schleusengraben 22,
21029 Hamburg, Germany
e-mail: oliver.menck@iwes.fraunhofer.de

Fatigue life calculation in bearings is an issue that has been the focus of decades of research culminating in national and international standards that are easily applicable to a wide variety of applications. However, almost all research has focused on simple, repetitive operating conditions. This paper explains why these approaches are not completely applicable to bearings under certain conditions, particularly not to those with a change in the load position over time undergoing inconstant movement. Based on existing standards, namely ISO 281, the paper then proposes a numerical approach to calculate the life of a bearing under stochastic operating conditions. The bearing life for any arbitrary load history and movement patterns can be calculated using the presented approach. The approach is presented and some example applications are given, notably including the life calculation of a rotor blade bearing in a wind turbine. [DOI: 10.1115/1.4055916]

Keywords: rolling contact, fatigue, numerical analysis, bearings, rolling element bearings

1 Introduction

Fatigue life calculation in bearings is a much studied topic that has been the focus of over a century of research [1]. Various different models have since been proposed, see Refs. [2,3] for an overview. Most influentially, Lundberg and Palmgren [4] published a model that continues to form the basis for most, if not all, national and international standards, most importantly ISO 281 [5]. Almost all of the research deals with bearings subjected to repetitive operating conditions. Their load is mostly constant or varies merely in magnitude, and their movement tends to be rotational or, in rare cases, oscillating with a constant oscillation angle that keeps repeating itself [6,7].

Bearings in some industrial applications do not adhere to these assumptions. Section 2 explains when these assumptions do not hold true. Notably, some bearings in wind turbines, such as yaw and pitch bearings, experience stochastic loads and movement patterns. Their load varies depending on wind conditions, not just in magnitude but also in direction. The movement of the bearing is determined by the pitch controller of the turbine, which adjusts the blade angle to control the power of the turbine and to reduce fatigue loading on other components of the turbine [8]. This leads to loads and movement as shown in Fig. 1, which is very much unlike anything seen in most typical industrial applications. Leupold et al. [10] proposed a segmentation of the bearing, which could presumably be used for such movement and loads, but use empirical S–N curves derived for merely one particular bearing.

This paper proposes a numerical approach to calculate the fatigue life of such bearings based on ISO 281 [5] and thus also Lundberg and Palmgren [4]. Based on a scalable rolling contact fatigue model from the two aforementioned references, a bearing is segmented. The cumulated damage of each segment over all operating conditions experienced by the bearing during its operating time is calculated first, and only thereafter are the individual segment damage cumulations combined to obtain one bearing life. This approach allows local changes in load magnitude and differences in the number of load cycles to be captured properly.

Some effects that can be modeled with the proposed approach have been considered in other publications. This includes some publications on oscillating bearings, notably Breslau and Schlecht [6] and Houpert and Menck [7], who derive analytical equations for an oscillating bearing in one invariable operating condition. The proposed approach in this paper can be considered as a generalized version of ISO 281 and the aforementioned publications. It hence leads to similar or identical results if identical operating conditions are assumed, but it can also be used for a wider variety of other conditions, most notably arbitrary timeseries of load magnitude, direction, and movement of the bearing.

The approach is explained in Sec. 3. Thereafter, some example applications are given in Sec. 4. These include a very simple load

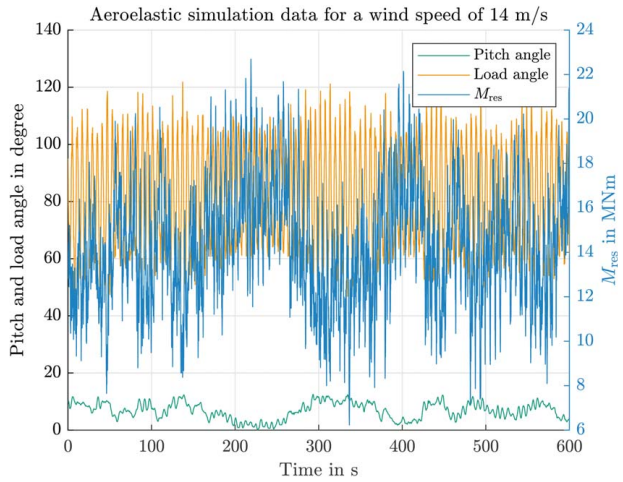

Fig. 1 Example rotor blade bearing movement and loads. Angle definitions according to Ref. [9].

Contributed by the Tribology Division of ASME for publication in the Journal of Tribology. Manuscript received May 31, 2022; final manuscript received September 5, 2022; published online November 17, 2022. Assoc. Editor: Nick Weinzapfel.

case, which is identical to the assumptions used by ISO 281 [5] and consequently leads to the same result, since the approach is derived from it. It also includes more advanced operating conditions which cannot be calculated purely with ISO 281, which are compared with other available literature. The Appendix gives a derivation of proportionality constant k required for Sec. 3 based on Lundberg and Palmgren [4] and ISO 281 [5].

2 The Palmgren–Miner Hypothesis Applied to the Entire Bearing

The Palmgren–Miner hypothesis was initially suggested by Palmgren in 1924 [11] to combine the effect of varying load levels in bearing life calculations mathematically. It has since found utilization in various applications, far exceeding just the use for bearings. However, the assumption that fatigue damage at all considered load levels occurs in the same position is implicit to the theory. As will be illustrated in the following, the application of the theory to an entire bearing life can therefore lead to erroneous outcomes.

2.1 Derivation of Palmgren–Miner Applied to the Entire Bearing. For a bearing experiencing a set of I operation conditions with $l_i : (i = 1 \ldots I)$ revolutions and corresponding lives $L_i = (C/P_i)^p$, using the Palmgren–Miner rule gives (cf. e.g., Harris and Kotzalas [12], "Effect of variable loading on fatigue life")

$$\frac{l_{\text{coll}}}{L_{\text{coll}}} = \sum_{i=1}^{I} \frac{l_i}{L_i} \tag{1}$$

Here, $l_{\text{coll}} = \sum_i^I l_i$ refers to the number of collective revolutions and L_{coll} refers to the corresponding life for the collective of operating conditions. Rearranging Eq. (1) for L_{coll} results in

$$L_{\text{coll}} = \left(\frac{1}{l_{\text{coll}}} \sum_{i=1}^{I} \frac{l_i}{L_i} \right)^{-1} \tag{2}$$

Replacing L_i and $L_{\text{coll}} = (C/P_{\text{coll}})^p$ and rearranging for P_{coll} results in

$$P_{\text{coll}} = \left(\frac{1}{l_{\text{coll}}} \sum_{i=1}^{I} l_i P_i^p \right)^{1/p} \tag{3}$$

Using the percentage of operating time q_i and the rotational speed n_i, and replacing $l_i/l_{\text{coll}} = q_i n_i / (\sum_{i=1}^{I} q_i n_i)$, Eq. (3) can also be displayed as

$$P_{\text{coll}} = \left(\frac{q_1 n_1 P_1^p + \cdots + q_I n_I P_I^p}{q_1 n_1 + \cdots + q_I n_I} \right)^{1/p} \tag{4}$$

This is a widespread equation that can be found in many manufacturer catalogs, e.g., Schaeffler Technologies AG & Co. KG [13], Liebherr-Components AG [14], and most basic machine element textbooks, see for instance Roloff et al. [15], Decker [16], or Haberhauer and Bodenstein [17] for a small selection.

2.2 Error/Simplification of Palmgren–Miner Applied to the Entire Bearing. Equation (1) and, subsequently, Eqs. (2) and (3) implicitly assume that the load distribution as well as the load cycles occur in the same position over all considered load levels. Moreover, they assume that the shape of the load distribution remains constant.

Lundberg and Palmgren [4] use a bottom-up approach in their calculation of fatigue life. In the event of uneven loading over the circumference of the bearing, as found in radial bearings or bearings subjected to a bending moment, they state: "The probability that the whole [···] ring will endure is the product of the probabilities that the different sections of the ring will endure".[1] Consequently, they take account of variable loads first on a local, segment-wise level and then combine individual segment lives into a total one[2] in their derivation of L.

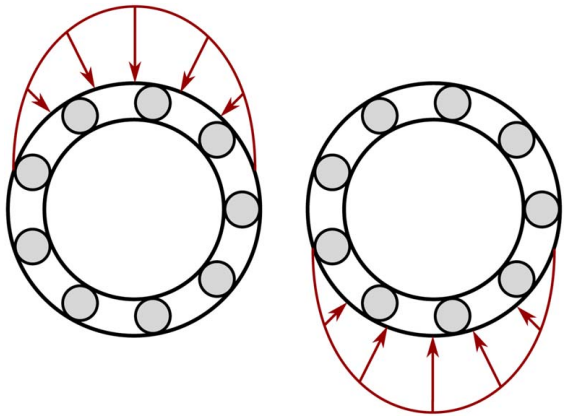

Fig. 2 Two load scenarios with the same life L

This very local consideration of loading is then what Eq. (1) is incapable of taking into account, since it works with lives L_i of an *entire* bearing. Variable L gives the life of a bearing in *one* constant condition, but can no longer give information about local effects of it. Operational changes that lead to a vastly different load situation can thus not be correctly captured. Figure 2 depicts two load scenarios that lead to the same life L. If the bearing condition were to change, causing it to operate in either scenario 50% of the time, Eqs. (1)–(3) would predict no change as compared to a constant load direction. This is obviously incorrect and it is a consequence of the loss of local information in the derivation of a bearing life L. This particular example has little impact on the life of a small, rotating bearing where the inner ring determines the life of the entire bearing, but for a large oscillating bearing, the influence is stronger.

Likewise, an oscillation that changes its mean position cannot correctly be calculated with the approach shown in Eq. (1). As the mean angle of the oscillation changes, different parts of the raceway are loaded, but the local information about this loading is lost in the calculation of a complete bearing life L. The NREL DG03 [19] recommends to correct for oscillation in its Eqs. (17)–(19), and then applies Palmgren–Miner to the entire bearing in its Eq. (22), even though the mean angle of oscillations will change in a typical blade bearing, thereby leading to the aforementioned problem.

Publications based on the DG03 as Schwack et al. [20] and Menck et al. [9] also apply Palmgren–Miner to the entire bearing, and thus suffer from related shortcomings. Similarly, Wöll et al. [21] propose a "Numerical Approach" for irregular operation conditions that applies Palmgren–Miner to the entire bearing and hence does not consider local effects properly.

Depending on the application, the influence of this effect varies. In many cases, the application of the Palmgren–Miner rule to the entire bearing will still give results very close to a more precise calculation, and in those cases, it can be considered a reasonable simplification. For other cases, notably for oscillating operation conditions or large bearings where the inner ring impacts the total

[1] Also known as Weibull weakest link theory according to Weibull [18].

[2] Note that this is an extremely simplified description. For survival probability S, Lundberg and Palmgren [4] start off with $\ln 1/S \sim (\tau_0^c N^e / z_0^h) V$. In the case of a pure thrust load, the raceway is evenly loaded and a segment-wise analysis is not required. Hence, in that case, V refers to the entire loaded volume of the raceway. Merely for uneven load distributions on the standing (typically outer) ring, they take the product of all individual survival probabilities, with $V \to \mathrm{d}V$. In rotating bearings, this is not needed for the rotating (typically inner) ring (even in the case of an uneven load distribution), since all segments of it experience the same load eventually.

bearing life more, the difference to a more precise calculation as shown in Sec. 3 may be stronger.

3 A Numerical Fatigue Life Model

The frequently cited starting point of the Lundberg–Palmgren theory [4] is

$$\ln\frac{1}{S} \sim \frac{\tau_0^c N^e}{z_0^h} V \tag{5}$$

where S refers to the survival probability of the bearing (or raceway) in question, τ_0 represents the maximum orthogonal shear stress occurring as a result of Hertzian contact pressure, and z_0 refers to the depth of this maximum shear stress under the surface. The volume[3] is given by V, and N denotes the number of stress cycles occurring in that volume by a passing rolling element. The variables c, e, and h are empirical parameters. A fourth empirical parameter k is needed to turn the proportionality given in Eq. (5) into an actual equation.[4]

For the purpose of this paper, each ring is split into M finite segments as depicted in Fig. 3. Equation (5) is thus turned into

$$\ln\frac{1}{S_m} = k\frac{\tau_{0,m}^c N_m^e}{z_{0,m}^h}\,\mathrm{d}V_m \tag{6}$$

for each segment m, where $\mathrm{d}V_m = a_m z_{0,m}\,(D_\mathrm{n}/2)\,d\psi$, with a_m being half the major axis of the Hertzian contact ellipse of segment m and D_n the raceway diameter (at the center of the contact). Variable k is a constant that will be determined from Lundberg and Palmgren [4] and adjusted according to ISO 281 in Appendix A of this paper.

3.1 Equivalent Loads Per Segment *m*. The novelty in the approach described herein lies in the application of the Palmgren–Miner rule *for each segment over all operating conditions* that occur over the operating time of the bearing. *Only thereafter* are the individual cumulated segment damages combined into a total bearing life L.

To this end, Eq. (6) is rearranged for N_m. We choose an arbitrary constant survival probability S_m and obtain for each segment m during a given load cycle n the relationship

$$\frac{1}{N_{m,n}} = \left(\frac{k}{\ln(1/S_m)}\frac{\tau_{0,m,n}^c}{z_{0,m,n}^h}\,\mathrm{d}V_{m,n}\right)^{1/e} \tag{7}$$

where $N_{m,n}$ denotes the number of cycles that segment m can withstand with survival probability S_m at the load occurring during load cycle n. Values $\tau_{0,m,n}$ and $z_{0,m,n}$ are determined as a function of said load for each segment $m = 1\ldots M$ and load cycle $n = 1\ldots n_m$. The loaded volume $\mathrm{d}V_{m,n}$ also varies for each segment and load cycle based on the major contact ellipse axis $a_{m,n}$ and $z_{0,m,n}$, both of which, too, result from the load acting in that load cycle.

This allows for application of the Palmgren–Miner rule for each segment m of the discretized ring as

$$\frac{n_m}{N_m} = \sum_{n=1}^{n_m}\frac{1}{N_{m,n}} \tag{8}$$

where N_m denotes the number of load cycles segment m can withstand with survival probability S_m for a representative collective of cycles $1\ldots n_m$. The number of cycles that actually occur is given by n_m. Implementing Eq. (7) and rearranging then gives

$$\ln\frac{1}{S_m} = k\underbrace{\left(\frac{1}{n_m}\sum_{n=1}^{n_m}\left(\frac{\tau_{0,m,n}^c}{z_{0,m,n}^h}\,\mathrm{d}V_{m,n}\right)^{1/e}\right)^e}_{=:\left(\tau_0^c\,\mathrm{d}V/z_0^h\right)_{m,\mathrm{eq}}} N_m^e \tag{9}$$

The equivalent ratio $\left(\tau_0^c\,\mathrm{d}V/z_0^h\right)_{m,\mathrm{eq}}$ gives an equivalent value of $\tau_0^c\,\mathrm{d}V/z_0^h$ over all occurring load cycles n of segment m. Setting $N_m = n_m$, we assume that the evaluated data contain 100% of operational time, and the values cancel out in Eq. (9). The value of S_m then gives the survival probability for the data set in question.

The time series may represent a condition that repeatedly occurs for x times, as is common in wind turbine simulations. In this case, the so-called multipliers x are applied to each load cycle n such that $x_n = x$ in a given time series. To this end, Eq. (9) needs to include multipliers in the values of $N_m = n_m = \sum_{n=1}^{n_m} x_n$ as well as in the sum $\left(\tau_0^c\,\mathrm{d}V/z_0^h\right)_{m,\mathrm{eq}} = \left((1/n_m)\sum_{n=1}^{n_m} x_n\left((\tau_{0,m,n}^c/z_{0,m,n}^h)\,\mathrm{d}V_{m,n}\right)^{1/e}\right)^e$.

3.2 Combining the Segments. "The probability that the whole $[\cdots]$ ring will endure is the product of the probabilities that the different sections of the ring will endure" [4]. Consequently, the survival probability S_r of a raceway is given by

$$\ln\frac{1}{S_r} = \sum_{m=1}^{M}\ln\frac{1}{S_m} \tag{10}$$

Combining R raceways into one bearing survival probability S_B is then mathematically identical

$$\ln\frac{1}{S_\mathrm{B}} = \sum_{r=1}^{R}\ln\frac{1}{S_r} \tag{11}$$

Note that Sec. 3.1 is merely concerned with one segmented ring. Survival probability S_m as per Eq. (9) will be different for segments on the inner and outer rings, even for the same number of segments M, due to differences in groove conformity, $\mathrm{d}V$, and most importantly relative differences of movement.

3.3 The Life *L*. Fatigue is most commonly measured in terms of life L_{10}, which corresponds to the point where the bearing retains a survival probability of 90 %, i.e., $S_\mathrm{B} = 0.9$. For ξ repetitions of some data set used in the above formulas, Eq. (9) gives the relation $\ln 1/S_m(\xi) \sim \xi^e$. This relation is retained throughout the application of Eqs. (10) and (11), giving

$$\ln\frac{1}{S_\mathrm{B}(\xi)} \sim \xi^e \tag{12}$$

The value received by application of Eq. (11) corresponds to $S_\mathrm{B}(\xi = 1)$. Thus, $\ln 1/S_\mathrm{B}(\xi) = \ln\,(1/S_\mathrm{B}(\xi = 1))\xi^e$ and for $S_\mathrm{B}(\xi) = 0.9$

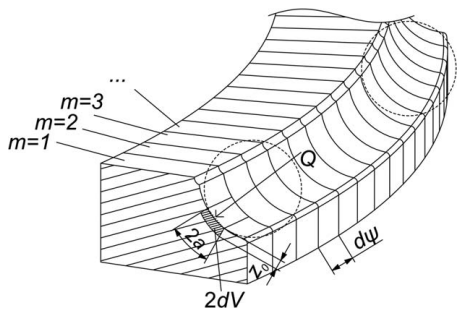

Fig. 3 Inner ring of a segmented bearing with nomenclature

[3] V is used here as $V = az_0l$, with l referring to the raceway circumference. Lundberg and Palmgren [4] merely define $V \sim az_0l$, and this paper uses a proportionality constant 1; this proportionality constant may be chosen arbitrarily as long as the constant k (here derived in the Appendix) is derived using the same definition.

[4] This publication uses parameters c, e, and h as given in DIN ISO [5] and derives k based on the same reference. However, other parameters could equally be used. The same principle could also be used for different life models as long as they are based on the Weibull weakest link theory.

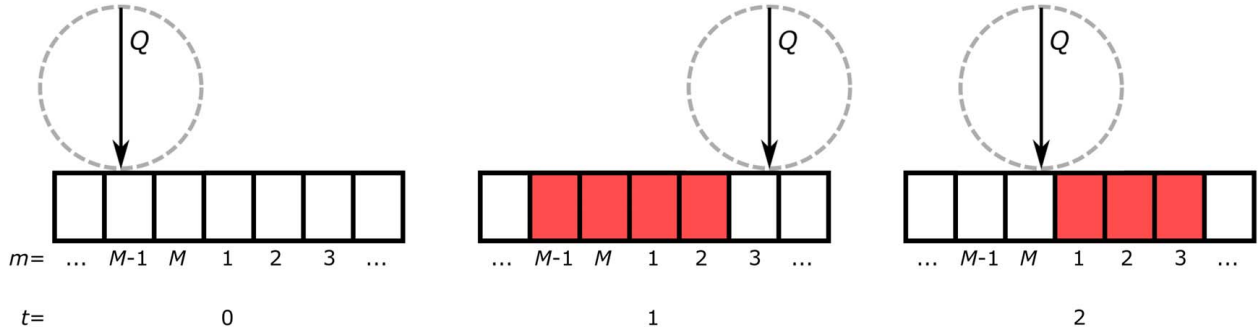

Fig. 4 Cycle definition used in this paper. Red segments experienced a load cycle in the respective step *t*

we find

$$\xi = \left(\log_{S_B(\xi=1)} 0.9\right)^{1/e} \tag{13}$$

Provided the data set used is of time T, we then finally obtain the life

$$L_{10} = \xi T = \left(\log_{S_B(\xi=1)} 0.9\right)^{1/e} T \tag{14}$$

Likewise, if the bearing makes some accumulated movement of D degrees during that time, the life in degrees of movement is given by $L_{10} = \xi D$. The variable ξ is hence a multiplier that tells how often the evaluated data set can be run until L_{10} is reached.

3.4 Further Details. In addition to the above mathematical derivations, some details remain to be defined.

For the determination of load cycles, the model analyzes the ball movement relative to each of the rings. For example, a movement θ_i of the inner ring with a stationary outer ring leads to a movement $\theta_c = 0.5 \cdot \theta_i \cdot (1 - \gamma)$ of the cage.[5] For a stationary outer ring, this can be seen to be the movement relative to the outer ring; however, relative to the moving inner ring, the movement of the cage is given by $\theta_i - \theta_c$. For each time-step of the simulation, and depending on the position of the cage, each ball's location with respect to the inner and outer segmentation is then respectively analyzed. No slippage of the rolling element set is assumed. The starting position of the first ball is chosen to be 0 deg, with the rest of the balls being evenly spaced accordingly.

A load cycle then occurs according to Fig. 4 for the definition used in this paper: it takes place in that step in which a segment is left. It does not matter on which side it entered, and it does not matter how long it resided in the segment, or if it resided at all. Therefore, shear stress τ_0 and depth z_0 used for some cycle n in Eq. (9) are given by the corresponding load Q in that time-step in which the segment is being left.

This definition of a load cycle does not follow directly from the Lundberg–Palmgren theory and one might also choose it differently, but the author expects differences from another load cycle definition (e.g., when a ball enters a segment) to be negligible for a sufficiently fine segmentation.

As in Lundberg and Palmgren [4] and ISO 281 [5], the order of loading is neglected by the given approach.

Moreover, the empirical exponents c, e, h, and the empirical parameter A used in the derivation of Lundberg and Palmgren [4] have to be defined. This publication follows the choice of ISO [5] which are mostly based on Ref. [4]. The values used herein are shown in Table 1 and the Appendix.

Lastly, Eq. (6) requires the variables τ_0, z_0, and a. For reasons of consistency, this paper employs the methods also used in Ref. [4]. The Hertzian contact is calculated by iteratively solving elliptical integrals by Hertz as given in Lundberg and Palmgren's Eq. (101), and the Hertzian contact is then defined by their Eq. (41). The variables z_0 and τ_0 are then obtained by solving their Eqs. (9) and (10). However, there are various other simplified methods to determine these values in the literature, including one by Houpert [22] and another one by Brewe and Hamrock [12]. These may be used as well, if desired, and will lead to similar, albeit not identical, results as the solution of the respective elliptical integrals. It is important to maintain the same Young's modulus and Poisson's ratio for the calculation of contact pressure and variable k in Eq. (A6).

4 Example Applications

Some example calculations are illustrated in the following. The approach can be used for any kind of movement in a bearing subjected to any kind of load history.

4.1 Simple Axial Bearing. For the basic case of a rotating, axially loaded bearing under a constant load and with a contact angle of 90 deg, the calculation can be simplified extremely. In this case, both the inner and outer rings are loaded identically. For a rotating bearing, the amount of load cycles can also be taken from the literature instead of being simulated as per Fig. 4. The amount is generally given by $u = Z/2 \cdot (1 \pm \gamma)$ load cycles per rotation, where Z is the number of balls and the upper sign (+) refers to the inner ring while the lower one (−) refers to the outer ring. For a contact angle of 90 deg, we obtain $\gamma = 0$. Thus, each position on the inner and outer ring experiences the same amount of load cycles $u = Z/2$.

We will use a ball bearing defined by $Z = 147$, pitch diameter $d_m = 4{,}690$ mm, ball diameter $D_a = 80$ mm, and groove conformity $f = 0.5319$. The bearing is loaded with $F_a = 10$ MN, which is assumed to spread evenly on the rolling elements,[6] giving a contact force of $Q = 68.03$ kN for each ball. Iteratively solving the Hertzian elliptical integrals and applying further equations by Ref. [4], this results in $\tau_0 = 559.57$ MPa and $z_0 = 0.749$ mm, $a = 9.45$ mm, and $l = \pi d_m$. With one rotation as reference, we obtain $N = u$. The constant $k = 1.441 \cdot 10^{-42}$ according to Eq. (A8).

Since the entire ring is evenly loaded and experiences the same amount of load cycles in every position, it is sufficient to use one 360 deg-wide segment.[7] Inserting the above values into Eq. (6) then returns $\ln(1/S_m) = 8.672 \cdot 10^{-7}$. Due to only using one segment, it follows from Eq. (10) that $\ln(1/S_r) = \ln(1/S_m)$. For the entire bearing, Eq. (11) gives $\ln(1/S_B) = 2 \cdot \ln(1/S_r)$. From

[5] γ is defined in the Nomenclature.

[6] It does not spread evenly in real applications, of course, hence why ISO includes $\lambda\eta$ in Eq. (A6).

[7] Of course, multiple segments could be used as well and would lead to the same result. Likewise, simulating the actual movement of the bearing and counting load cycles as described in Sec. 3.4 would (approximately) lead to the same result as assuming $N = Z/2$ for one rotation.

Table 1 Exponents *c*, *e*, *h*, and *p* according to ISO, and the resulting *k*

	c	*e*	*h*	*p*	*k*
Point contact	31/3	10/9	7/3	3	see Eq. (A8)

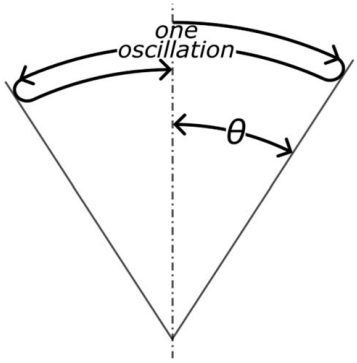

Fig. 5 Oscillation amplitude θ

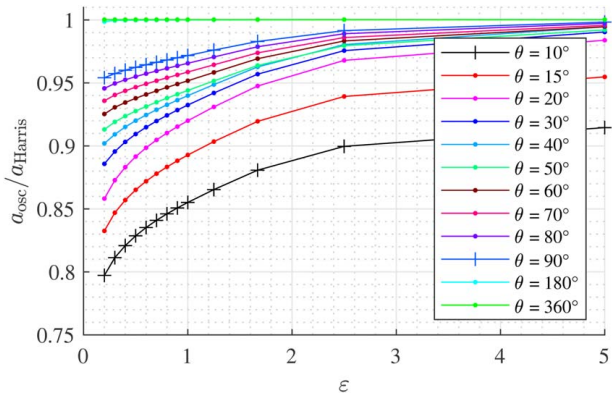

Fig. 6 Oscillation factors derived from simulations of a 7220 type bearing

Eq. (13) it follows that $\xi = 20{,}192$. Since the input data used corresponds to one revolution, it follows that $L_{10} = 20{,}192$ rev.

Applying Eq. (A6) for the above bearing, we obtain $C_a = 2.723$ MN. The life calculated according to Ref. [5] thus results in $L_{10} = (C_a/F_a)^3 \cdot 10^6 = 20{,}192$ rev, which is identical to the result calculated above. This is due to the simple load case considered, which corresponds exactly to the assumptions used by Lundberg and Palmgren [4] and, by extension, ISO [5].

4.2 Oscillating Bearing. Oscillating bearings have been considered analytically in the literature based on modifications of the Lundberg–Palmgren theory. Notably, Breslau and Schlecht [6] and Houpert and Menck [7] published approaches to correct the standard ISO life for oscillation. The same is possible with the numerical model presented here, as it is presented in Sec. 3.

To this end, simulations have been performed to reproduce the results of Houpert and Menck [7] using the model presented in this paper. An entire ball bearing, consisting of an inner and outer ring,[8] has been simulated. A 7220 type bearing with 15 balls of diameter $D_a = 25.4$ mm and a contact angle of $\alpha = 45$ deg was used to this end. Inner and outer ring were each divided into 1,800 segments. One oscillation of θ degrees amplitude was performed using the same angle definition as in the aforementioned reference, shown in Fig. 5, for a variety of θ. At the same time, a load zone as in the given reference was used (identical to that one used by Lundberg and Palmgren [4]) and is described by the value ε. Simulations have been performed for the same values of ε as in the reference to obtain $L_{10,\mathrm{osc}}$. For each value of ε, one rotation was performed as well to obtain $L_{10,\mathrm{rot}}$. Then, an oscillation factor was calculated according to $a_{\mathrm{osc}} = L_{10,\mathrm{osc}}/L_{10,\mathrm{rot}}$, which was then further divided by the so-called Harris factor $a_{\mathrm{Harris}} = 90/\theta$ for improved display.

The results are shown in Fig. 6. When comparing Figs. 6–10 of Houpert and Menck [7], the factor given here is below that shown by Houpert and Menck [7] for small oscillations. This is because the simulations performed in here automatically include an effect not yet considered in the given reference: With oscillations below the critical angle $\theta_{\mathrm{crit}} = 2\pi/(Z\,(1 \pm \gamma))$, only a part of the raceway is loaded. This leads to an additional effect on the life, which Houpert and Menck [7] introduce only after showing their[9] Fig. 10. That is to say the simulations performed with the model shown in this paper automatically include in their results all relevant effects that occur when any kind of oscillation, small or large, is performed. The user does not require advanced understanding of any effects that arise for any specific type of movement, neither do they have to derive lengthy equations for any number of effects that arise; as long as the actual movement and loads are included in the input data for the model, their effects are automatically included.

4.3 Application of the Methods to a Rotor Blade Bearing. Rotor blade bearings are subject to stochastic external conditions from the wind, and their load and movement thus cannot be described analytically. An example of rotor blade movement and loads is given in Fig. 1. This is hence where the approach herein can be used to calculate a correct solution based on the assumption made by Lundberg and Palmgren [4] as shown in Eq. (5). The method described in Sec. 3 is thus applied to DLC1.1 time series data given in Ref. [24] and determined according to IEC 61400-1 [25]. This contains simulated load series based on stochastic wind conditions that are assumed to be Weibull distributed according to IEC [25] for wind turbine class IA. The same time series have also been used in the life calculation in Menck et al. [9]. The data are made up of 50 ms time-steps and each time-step is analyzed for load cycles resulting from movement of the bearing, which are then added according to Sec. 3.1. The bearing, too, is identical to that one in the aforementioned publication. It is a double-row four-point bearing with four inner and outer raceways, respectively. The raceways are called 1A, 1B, 2A, and 2B. For a sketch of the bearing, see Ref. [9].

The life of the bearing is calculated according to Sec. 3.2. The contact forces Q are calculated based on finite element simulations according to Menck et al. [9], and τ_0, z_0, and a are calculated according to Lundberg and Palmgren [4]. Variable $k = 9.1396 \cdot 10^{-43}$ according to Appendix A. A convergence analysis was performed and resulted in <0.1 % change for more than $M = 1800$ segments, which is thus the number used for the simulations.

Twenty years of operation have been simulated with 255 10-min bins under different wind speeds and with multipliers corresponding to the respective percentage of the wind speed in question. As a measure of damage, the value $\ln(1/S_m)$ after 20 years of operation is displayed in Fig. 7. Each dot in the figure corresponds to a segment. The results of two segments right next to each other can vary considerably. This is particularly due to the large number of

[8]All calculations in this paper include the inner and outer ring. This is only emphasized here because Ref. [7] also includes a separate calculation for each ring.

[9]The effect is included in Houpert and Menck [7], Section 4.4, with the factor $f_{\theta\_\mathrm{crit\_i,o}}$ in their Eq. (45), which has to be applied to the oscillation factors given in their Fig. 10 in order to obtain Fig. 6 of this paper. Further slight deviations may occur because Houpert and Menck [7] use the model by Dominik [23] and adjust it for point contact, giving very similar but not identical results to the model by Lundberg and Palmgren [4], and because possible interdependence of various effects that occur is more accurately captured in the model presented in this paper.

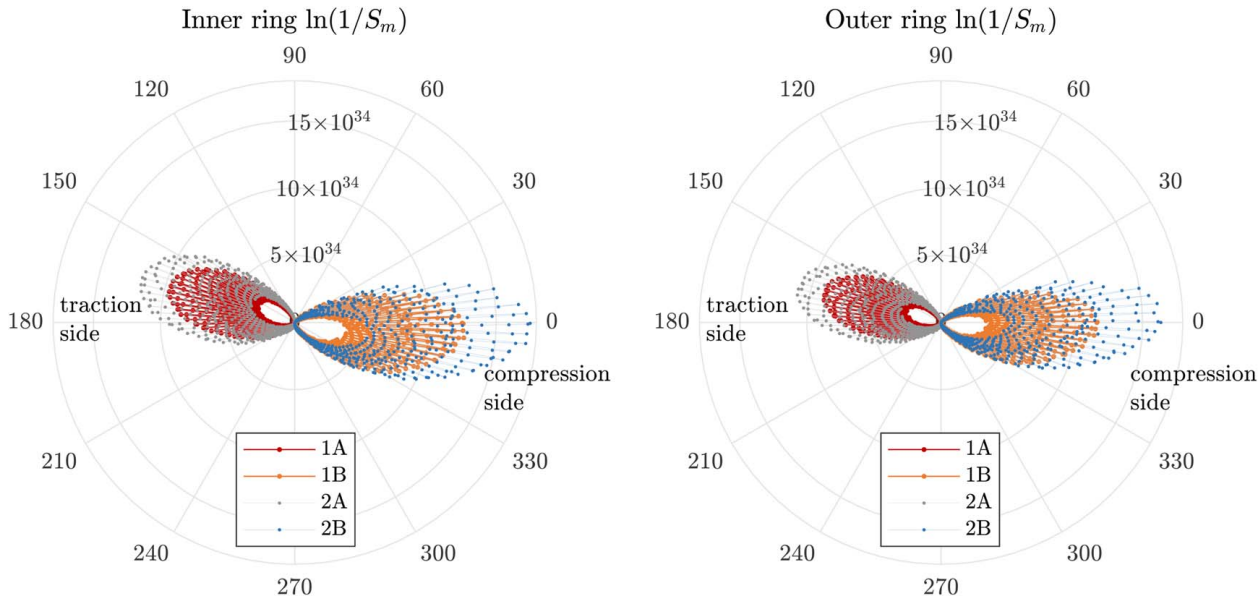

Fig. 7 $\ln(1/S_m)$ of the raceways in a rotor blade bearing for $M = 1800$ segments after 20 years of turbine operation. Raceway definitions according to Ref. [9]: Raceways 1 are near the wind turbine hub (zoom in on the image for a better view), and raceways 2 are near the rotor blade. Raceways B are loaded on the compression side of the bearing (0 deg region), and raceways A are loaded on the traction side (180 deg region).

balls in each row of the bearing ($Z = 147$) and the small movements that it performs during operation, which means balls tend to stay within a few segments.

The resulting life is $L_{10} = 858.54$ days. This can be compared to the result obtained in Menck et al. [9], which gives a modified reference life of $L_{10\,\mathrm{m}} = 2520$ h or 105 days. $L_{10\,\mathrm{m}}$ includes the lubrication factor $a_{\mathrm{ISO}} \approx 0.1$, correcting for which results in a life of $L_{10} = 1050$ days. This is 22% above the result calculated herein, particularly because Menck et al. [9] did not correct for the influence of oscillation on the life. However, even though the aforementioned publication uses Palmgren–Miner applied to the entire bearing which, as stated in Sec. 2, is not correct, the results are reasonably similar. One influence on the relatively small difference is the Weibull slope of $e = 1.1$ according to Table 1, which is very close to 1. Other authors [1,23] have suggested values for e that differ more from 1, which would result in higher differences between the life calculated from a "global" application of the Palmgren–Miner hypothesis as shown in Sec. 2 and the more accurate "local" application of the finite segment method as shown in Sec. 3 and as used for the results shown here. Lastly, despite the change in the direction of the resulting moment, one can see in Fig. 7 that most of the damage occurs merely within a range of about 60 deg on the compression and the traction side, which means that the change of load direction is not as big as, for example, depicted in the more extreme example of Fig. 2 for this particular case.

5 Conclusions

The paper showed that the application of the Palmgren–Miner hypothesis to the lives of entire bearings can lead to incorrect results if the qualitative position of the load changes, either by a change of the global load direction or by small, nonrepetitive movement that leads to load cycles occurring in different locations. A numerical model was proposed that accounts for variations in the local load cycle position and magnitude for arbitrary time-varying movement and load angles. For the same assumptions as taken by Lundberg and Palmgren [4] (e.g., constant load direction, full rotations, same load zone, Hertzian rolling elements) and consequently ISO 281 [5], the model has been shown to produce identical results to ISO as well as a publication on oscillating bearings by Houpert and Menck [7]. The model was then applied to a rotor blade bearing which undergoes effectively random small oscillations and load changes due to the wind. The effect of this was analyzed and compared to an earlier publication by Menck et al. [9] that applied Palmgren–Miner to the entire blade bearing. Even though doing so is not entirely accurate, as shown in this publication, the results are reasonably similar.

Acknowledgment

Thanks to Iman Talai for implementing the model outlined in an earlier version of this paper, and thanks to Matthias Stammler for proofreading the paper.

Funding Data

- The German Federal Ministry for Economic Affairs and Climate Action (Grant reference numbers 0324344A and 03EE2033A).

Nomenclature

a = half major contact ellipse axis, mm
c = empirical exponent
e = Weibull slope
f = groove conformity
h = empirical exponent
i = index of an operating condition
k = proportionality constant, *for other variables using N and mm*
l = number of revolutions; *also:* raceway circumference, mm
m = index of a finite segment
n = index of a load cycle; *also:* rotational speed, 1/min
p = load-life exponent
q = percentage of operating time, %
r = index of a raceway
u = load cycles per rotation

x = time series multiplier
A = empirical parameter
C = load rating, N
D = accumulated movement, deg
I = number of operating conditions
L = life, (10^6) revolutions
M = number of finite segments
N = number of load cycles
P = equivalent load, N
Q = rolling body load, N
R = number of raceways
S = survival probability
T = duration of time series, s
V = loaded volume, mm^3
Z = number of balls
a_{osc}, a_{Harris} = corrective factors for oscillation
d_m = pitch diameter, mm
dV = loaded volume of a finite segment, mm^3
l_{coll} = collective number of revolutions
z_0 = depth of τ_0, mm
D_a = ball diameter, mm
D_n = raceway diameter, mm
F_a = axial force, N
L_{coll} = collective life, (10^6) revolutions
L_{10} = life with $S = 0.9$, (10^6) rev, days
L_{10m} = modified reference life, (10^6) rev, days, h
M_{res} = resulting bending moment, MNm
P_{coll} = collective equivalent load, N
S_B = bearing survival probability

Greek Symbols

α = contact angle, deg
γ = auxiliary value $D_a \cos(\alpha)/d_m$
ε = load zone parameter
θ = oscillation angle, deg
θ_i = inner ring angle, deg
θ_c = cage angle, deg
ξ = life multiplier
τ_0 = max. orthogonal shear stress, MPa
$d\psi$ = width of finite segment, rad

Appendix: Derivation of k

The following derivation is heavily based on the original work of Lundberg and Palmgren [4] (termed "LP" in the following) and cannot be completely understood without it. The equations that follow thus use the same nomenclature as LP and their variables are not explained in the following. Furthermore, most explanations given in the original work are skipped here. The focus lies on using the same equations as LP, but with inclusion of a variable k from the very beginning in order to obtain an equation as shown in Eq. (6) rather than merely a proportionality as given in Eq. (5). Harris and Kotzalas [12] give an overview over the calculation with similar, albeit not identical, nomenclature and may be used to follow the equations as well.

Equations from the original work of Lundberg and Palmgren [4] are labeled "LP." Differences due to the derivation of k are highlighted in red (see color equations online).

A.1 Derivation of Basic k. The starting point is Eq. (5). This corresponds to LP's Eq. (37), but here a factor k is included to obtain an equation

$$\ln\frac{1}{S} = k\frac{\tau_0^c N^e}{z_0^h}V \qquad \text{(LP 37)}$$

Introducing $V = az_0l$, $\tau_0 = Tq$, $z_0 = zb$, and $q = 3\,Q/(2\pi ab)$, and, after rearranging, we obtain

$$\ln\frac{1}{S} = k\left(\frac{3}{2\pi}\right)^c \frac{T^c a l}{(\zeta b)^{h-1}} N^e \left(\frac{Q}{ab}\right)^c \qquad \text{(LP 39)}$$

The above equation is thus identical to LP's Eq. (39) but includes the red term $k\left(\frac{3}{2\pi}\right)^c$, which is neglected by LP because it is constant and they maintain a proportionality rather than an equation.

Next, we introduce $N = uL$, $l = \pi D_n$, and Eq. (LP 41) into the above equation. Furthermore, the unity $1 = D_a^{(c+h-1)/2} D_a^{(c-h-1)/2} D_a^{-(c-h+1)} D_a^{2-h}$ is multiplied with the equation. We rearrange to obtain

$$\ln\frac{1}{S} = k\left(\frac{3}{2\pi}\right)^c \pi \frac{T^c}{\zeta^{h-1}}\left(\frac{E_0 D_a \sum\rho}{3\mu\nu^2}\right)^{(c+h-1)/2}\left(\frac{D_a}{a}\right)^{(c-h-1)/2} \cdot \left(\frac{Q}{D_a^2}\right)^{(c-h+1)/2} D_n D_a^{2-h} u^e L^e \qquad \text{(LP 43)}$$

Note that only an additional π, from the inclusion of $l = \pi D_n$, has joined the red term. This is because most values introduced are variable, though some are constant and will subsequently be added to the red term.

The above equation holds true for line as well as point contact. Adding now the Hertzian relationship for a under **point contact**, cf. Eq. (LP 41), results in

$$\ln\frac{1}{S} = k\left(\frac{3}{2\pi}\right)^c \pi \frac{T^c}{\zeta^{h-1}\mu^{c-1}\nu^{c+h-1}}\left(\frac{E_0 D_a \sum\rho}{3}\right)^{(2c+h-2)/3} \cdot \left(\frac{Q}{D_a^2}\right)^{(c-h+2)/2} D_n D_a^{2-h} u^e L^e \qquad \text{(LP 44)}$$

with no change in the red term. The unities $(T_1/T_1)^c$ and $(\zeta_1/\zeta_1)^{h-1}$ are then multiplied with the above equation, and it is rearranged to give

$$\frac{Q}{D_a^2} L^{3e/(c-h+2)} = \left[\ln\frac{1}{S}\left\{k\left(\frac{3}{2\pi}\right)^c \pi \frac{T_1^c}{\zeta_1^{h-1}}\left(\frac{E_0}{3}\right)^{(2c+h-2)/3}\right\}^{-1}\right]^{3/(c-h+2)} \cdot \Phi D_a^{-3(3-h)/(c-h+2)} \qquad \text{(LP 47)}$$

where Φ includes a number of values and is defined in Eqs. (LP 49) and (LP 59). In Eq. (LP 47), LP finally introduce an empirical proportionality constant A_1 to obtain an equation. Comparing the above equation to LP's Eq. (47), it is evident that the red term to the left of Φ is identical to A_1, thereby resulting in

$$\left[\ln\frac{1}{S}\left\{k\left(\frac{3}{2\pi}\right)^c \pi \frac{T_1^c}{\zeta_1^{h-1}}\left(\frac{E_0}{3}\right)^{(2c+h-2)/3}\right\}^{-1}\right]^{3/(c-h+2)} = A_1$$

Rearranging finally gives k as

$$k = \ln\frac{1}{S}\left\{\left(\frac{3}{2\pi}\right)^c \pi \frac{T_1^c}{\zeta_1^{h-1}}\left(\frac{E_0}{3}\right)^{(2c+h-2)/3}\right\}^{-1} A_1^{-(c-h+2)/3} \qquad \text{(A1)}$$

This equation can be used to obtain a life in *millions* of revolutions (or millions of any other kind of movement occurring in the data). In order to obtain the life in *single* revolutions (or single instances of any other kind of movement), the above equation is to be multiplied by 10^{-6e}.

With the constants c, e, and h as given in Table 1, and knowing that the constants have been derived for a survival probability $S = 0.9$, the equation reduces to

$$k = 9.0255 \cdot 10^{-27} A_1^{-10/3} \quad \text{for millions of movements or}$$
$$k = 1.9445 \cdot 10^{-33} A_1^{-10/3} \quad \text{for single movements} \qquad \text{(A2)}$$

if N and mm are used as units. E_0 has been calculated according to Eq. (LP 40) assuming a Young's modulus of $E = 210$ GPa and Poisson's ratio 0.3, and T_1 and ζ_1 have been used according to LP's Table 1.

A.2 Derivation of A_1. In the following, the derivation of the load rating C will be undertaken in order to determine A_1. Following the derivation by LP, the constant A_1 is simply replaced by $A = 0.089 \cdot A_1$, with $A = 98.0665$ according to DIN [26] if N and mm are used as units.[10] However, further additions made at the end of the derivation of the load rating C are not included in the aforementioned definition of A_1. Particularly ISO [5] has made several adjustments to the load rating following the original derivation by LP, and in the following we will use A_1 to include any and all adjustments made to the load rating up until its final form as given in ISO 281.

The load rating for both the inner (i) and outer (e) ring is defined as

$$C_{i,e} = Q_{ci,e} Z \sin\alpha \tag{LP 80}$$

Q_c is defined as the value of Q at[11] $L = 1$. Rearranging Eq. (LP 47) results in $Q_c = A_1 \Phi D_a^{1.8}$ and hence the above equation turns into

$$C_{i,e} = A_1 \Phi_{i,e} D_a^{1.8} Z \sin\alpha \tag{A3}$$

Now, LP change Φ to be more usable for general calculations. This includes a number of steps skipped here, and results in LP's Eq. (108), which gives

$$\Phi = 0.06855\ \omega\ \frac{[1\mp\gamma]^{1.8}}{[1\pm\gamma]^{1/3}} \left(\frac{D_a}{d_m}\right)^{0.3} Z^{-1/3}$$
$$\omega = [1 + F(b/a)]^{2.1} \left[\frac{T_1}{T}\right]^{3.1} \left[\frac{\zeta}{\zeta_1}\right]^{0.4} \mu^{2.8} \nu^{3.5} \tag{LP 108}$$

where $\gamma = D_a \cos\alpha / d_m$, $F(b/a)$ is a function defined in Eq. (LP 100), and the upper sign in $\mp$ and $\pm$ refers to the inner and the lower one to the outer ring.

The above ω includes Hertzian values μ and ν, which are obtained by iteratively solving elliptical integrals given in Eq. (LP 101). This is easily achieved with the aid of modern computing, but LP used a term to approximate ω instead as

$$\omega \approx 1.3\ \Omega^{-0.41} = 1.3 \left[\frac{2R}{D_a} \frac{r}{r - R}\right]^{0.41} [1 \mp \gamma]^{-0.41} \tag{LP 109}$$

We therefore introduce the simplification as done by LP, but include a term in red for the slight error caused by this assumption and obtain

$$\Phi = 0.06855\ \frac{\omega}{1.3\ \Omega^{-0.41}}\ 1.3\ \Omega^{-0.41}\ \frac{[1\mp\gamma]^{1.8}}{[1\pm\gamma]^{1/3}} \left(\frac{D_a}{d_m}\right)^{0.3} Z^{-1/3}$$

A slight rounding error obtained by introducing 0.06855 is neglected here as it makes for less than 0.1% of difference in the final life. The red term $\omega/(1.3\ \Omega^{-0.41})$ is approximately 1, but off by a few percent depending on the bearing in question.

Introducing the above into Eq. (A3) hence results in

$$C_{i,e} = \frac{\omega}{1.3\ \Omega^{-0.41}}\ 0.089115\ A_1\ \Omega^{-0.41}\ \frac{[1\mp\gamma]^{1.8}}{[1\pm\gamma]^{1/3}} \left(\frac{D_a}{d_m}\right)^{0.3} \cdot Z^{-1/3} D_a^{1.8} Z \sin\alpha \tag{A4}$$

where only ω and Ω differ between the inner and outer ring, and as usual the upper sign of $\mp$ and $\pm$ refers to the inner ring whereas the lower one refers to the outer ring.

To obtain a final load rating, we then apply LP's Eq. (87)

$$C = \left[1 + \left(\frac{C_i}{C_e}\right)^{pe}\right]^{-1/pe} C_i \tag{LP 87}$$

with $p = (c - h + 1)/2e$ as per Eq. (LP 55) resulting in $pe = 10/3$. The ratio C_i/C_e is technically dependent on the red term in Eq. (A4), but the influence on the final life is tiny ($\ll 0.1\%$) and thus neglected here. Introducing Eq. (A4) into Eq. (LP 87), knowing that for ball bearings $2R = D_a$, and rearranging, thus gives finally the load rating according to LP as

$$C = \frac{\omega_i}{1.3\ \Omega_i^{-0.41}}\ 0.089115\ A_1 \left[\frac{2r_i}{2r_i - D_a}\right]^{0.41} \gamma^{0.3} \frac{[1-\gamma]^{1.39}}{[1+\gamma]^{1/3}} \cdot \left[1 + \left\{\left[\frac{r_i}{r_e}\left(\frac{2r_e - D_a}{2r_i - D_a}\right)\right]^{0.41} \left(\frac{1-\gamma}{1+\gamma}\right)^{1.72}\right\}^{10/3}\right]^{-3/10} \cdot (\cos\alpha)^{0.7} \tan\alpha\ Z^{2/3}\ D_a^{1.8} \tag{A5}$$

where the subscript i refers to values of the inner and e to values of the outer ring. Again, a slight but negligible rounding error is observed by the introduction of 1.72 rather than the exact value of $1.72\overline{3}$.

The load rating in Eq. (A5) can be compared to the axial load rating given in Ref. [5] using Ref. [26]. Blue terms ($b_m\ 98.0665\ \lambda\ \eta$ for $D_a \le 25.4$ mm and $3.647\ b_m\ 98.0665\ \lambda\ \eta\ D_a^{1.4}$ for $D_a > 25.4$ mm) deviate from Eq. (A5) (see color equations online):

$$C_a = b_m\ 98.0665\ \lambda\ \eta \left[\frac{2r_i}{2r_i - D_a}\right]^{0.41} \gamma^{0.3} \frac{[1-\gamma]^{1.39}}{[1+\gamma]^{1/3}} \cdot \left[1 + \left\{\left[\frac{r_i}{r_e}\left(\frac{2r_e - D_a}{2r_i - D_a}\right)\right]^{0.41} \left(\frac{1-\gamma}{1+\gamma}\right)^{1.72}\right\}^{10/3}\right]^{-3/10} \cdot (\cos\alpha)^{0.7} \tan\alpha\ Z^{2/3}\ D_a^{1.8} \quad \text{for } D_a \le 25.4\,\text{mm}$$
$$C_a = 3.647\ b_m\ 98.0665\ \lambda\ \eta \left[\frac{2r_i}{2r_i - D_a}\right]^{0.41} \gamma^{0.3} \frac{[1-\gamma]^{1.39}}{[1+\gamma]^{1/3}} \cdot \left[1 + \left\{\left[\frac{r_i}{r_e}\left(\frac{2r_e - D_a}{2r_i - D_a}\right)\right]^{0.41} \left(\frac{1-\gamma}{1+\gamma}\right)^{1.72}\right\}^{10/3}\right]^{-3/10} \cdot (\cos\alpha)^{0.7} \tan\alpha\ Z^{2/3}\ D_a^{1.4} \quad \text{for } D_a > 25.4\,\text{mm} \tag{A6}$$

Comparing Eq. (A5) with Eq. (A6), we then finally obtain A_1 as

$$A_1 = \frac{b_m\ 98.0665\ \lambda\ \eta}{0.089115} \frac{1.3\ \Omega_i^{-0.41}}{\omega_i} \quad \text{for } D_a \le 25.4\,\text{mm}$$
$$A_1 = 3.647\ \frac{b_m\ 98.0665\ \lambda\ \eta}{0.089115} \frac{1.3\ \Omega_i^{-0.41}}{\omega_i} D_a^{-0.4} \quad \text{for } D_a > 25.4\,\text{mm} \tag{A7}$$

where $b_m = 1.3$ according to Ref. [5], $\lambda = 0.9$ and $\eta = 1 - \sin(\alpha)/3$ according to Ref. [26] for axial ball bearings. All the given derivations also apply for radial ball bearings, but they contain different values for b_m, λ, and η, see Ref. [26].

A.3 Final k. Finally, combining Eq. (A2) with Eq. (A7), we obtain for the case of single movements in ball bearings, using N and mm,

$$k = 1.4133 \cdot 10^{-43} \left(b_m\ \lambda\ \eta \frac{1.3\ \Omega_i^{-0.41}}{\omega_i}\right)^{-10/3} \quad \text{for } D_a \le 25.4\,\text{mm}$$
$$k = 1.8929 \cdot 10^{-45} \left(b_m\ \lambda\ \eta \frac{1.3\ \Omega_i^{-0.41}}{\omega_i} D_a^{-0.4}\right)^{-10/3} \quad \text{for } D_a > 25.4\,\text{mm} \tag{A8}$$

[10] LP use kg and mm as units, in which case $A = 10$.

[11] $L = 1$ is the value used by LP to refer to a million revolutions. It thus corresponds to the upper part of Eq. (A7). The lower part of Eq. (A7) can be used to correct for the assumption of a million revolutions (movements) and instead obtain a life in single revolutions (movements).

Since calculation of the term $1.3\,\Omega_i^{-0.41}/\omega_i$ is laborious, it may be assumed to be 1 within reasonable accuracy, though all calculations in this paper include it.[12] Values b_m, λ, and η are chosen according to the bearing type in question as per Ref. [26]; for axial ball bearings, $b_m\,\lambda\,\eta = 1.17 \cdot (1 - \sin(\alpha)/3)$, where α is the contact angle. Variable D_a is the ball diameter in mm.

Conflict of Interest

There are no conflicts of interest.

Data Availability Statement

The authors attest that all data for this study are included in the paper.

References

[1] Zaretsky, E. V., 2013, Rolling Bearing Life Prediction, Theory, and Application: NASA/TP—2013-215305. https://ntrs.nasa.gov/citations/20160013905.

[2] Sadeghi, F., Jalalahmadi, B., Slack, T. S., Raje, N., and Arakere, N. K., 2009, "A Review of Rolling Contact Fatigue," ASME J. Tribol., **131**(4), p. 041013.

[3] Tallian, T. E., 1992, "Simplified Contact Fatigue Life Prediction Model—Part I: Review of Published Models," ASME J. Tribol., **114**(2), pp. 207–213.

[4] Lundberg, G., and Palmgren, A., 1947, "Dynamic Capacity of Rolling Bearings," Proceedings of the Royal Swedish Academy of Engineering Sciences, No. 196, Generalstabens Litografiska Anstalts Förlag, Stockholm.

[5] DIN ISO, 2010, DIN ISO 281:2010-10, "Rolling Bearings – Dynamic Load Ratings and Rating Life" (ISO 281:2007).

[6] Breslau, G., and Schlecht, B., 2020, "A Fatigue Life Model for Roller Bearings in Oscillatory Applications," Bearing World J., **5**, pp. 65–80. https://d-nb.info/1233208187/34#page=65.

[7] Houpert, L., and Menck, O., 2022, "Bearing Life Calculations in Rotating and Oscillating Applications," ASME J. Tribol., **144**(7), p. 071601.

[8] Burton, T., Jenkins, N., Sharpe, D., and Bossanyi, E., 2011, *Wind Energy Handbook*, 2nd ed., Wiley, Chichester, West Sussex.

[9] Menck, O., Stammler, M., and Schleich, F., 2020, "Fatigue Lifetime Calculation of Wind Turbine Blade Bearings Considering Blade-Dependent Load Distribution," Wind Energy Sci., **5**(4), pp. 1743–1754.

[10] Leupold, S., Schelenz, R., and Jacobs, G., 2021, "Method to Determine the Local Load Cycles of a Blade Bearing Using Flexible Multi-Body Simulation," Forschung im Ingenieurwesen, **85**(2), pp. 211–218.

[11] Zaretsky, E. V., 1997, "A. Palmgren Revisited—A Basis for Bearing Life Prediction," NASA Technical Memorandum 107440. https://ntrs.nasa.gov/citations/19970025228.

[12] Harris, T. A., and Kotzalas, M. N., 2007, *Rolling Bearing Analysis*, 5th ed., Taylor & Francis, Boca Raton, FL.

[13] Schaeffler Technologies AG & Co. KG, 2019, "Rolling Bearings, Catalogue (HR 1)," Order Number 029679141-0000.

[14] Liebherr-Components AG, 2017, Product Catalogue Slewing Bearings.

[15] Roloff, H., Matek, W., and Wittel, H., 1987, *Maschinenelemente: Normung, Berechnung, Gestaltung* (Viewegs Fachbücher der Technik. 11.), durchges. Aufl. ed., Vieweg, Braunschweig.

[16] Decker, K. H., 1995, *Maschinenelemente* (Das Fachwissen der Technik. 12.), überarb.u. erw. Aufl. ed., Hanser, München.

[17] Haberhauer, H., and Bodenstein, F., 2001, *Maschinenelemente: Gestaltung, Berechnung, Anwendung: Mit 108 Tabellen* (Springer-Lehrbuch. 11.), vollst. überarb. Aufl. ed., Springer, Berlin, Heidelberg.

[18] Weibull, W., 1939, "A Statistical Theory of the Strength of Materials," Ingeniörsvetenskapsakademiens handlingar.

[19] Harris, T., Rumbarger, J. H., and Butterfield, C. P., 2009, "Wind Turbine Design Guideline DG03: Yaw and Pitch Rolling Bearing Life," United States.

[20] Schwack, F., Stammler, M., Poll, G., and Reuter, A., 2016, "Comparison of Life Calculations for Oscillating Bearings Considering Individual Pitch Control in Wind Turbines," J. Phys. Conf. Ser., **753**(11), p. 112013.

[21] Wöll, L., Jacobs, G., and Kramer, A., 2018, "Lifetime Calculation of Irregularly Oscillating Bearings in Offshore Winches," Modeling Identification Control: A Norwegian Research Bull., **39**(2), pp. 61–72.

[22] Houpert, L., 2001, "An Engineering Approach to Hertzian Contact Elasticity—Part I," ASME J. Tribol., **123**(3), pp. 582–588.

[23] Dominik, W. K., 1984, "Rating and Life Formulas for Tapered Roller Bearings," SAE Technical Paper Series, SAE International 400 Commonwealth Drive, Warrendale, PA, 10.4271/841121.

[24] Popko, W., 2019, "Aero-Elastic Simulation Time Series of IWT7.5 Reference Turbine," 10.24406/fordatis/113.

[25] IEC, 2005, IEC 61400-1:2005-08: "Wind Turbines – Part 1: Design Requirements."

[26] DIN, Wälzlager – Erläuternde Anmerkungen zur ISO 281 – Teil 1: Dynamische Tragzahlen und nominelle Lebensdauer (ISO/TR 1281-1:2008 + Cor. 1:2009).

[12]Internal calculations not included in this paper have produced about 10% discrepancy in the calculated life without the term in question. As shown in Sec. 4.1, inclusion of the term virtually removes any difference to the standard for simple reference load cases.